Insights into Fault Zone Architecture and Growth Based on Enhanced Image of Fault Zone Arrays Using Hybrid Attributes

Lijie Cui, Dandan Dong, Yawen huang

(Petroleum Institute, China University of Petroleum-Beijing at Karamay, Karamay, Xinjiang, China, 834000)

Introduction

The fault zone architecture is very complex, generally consisting of fault cores and surrounding damage zones (Caine et al., 1996) with different permeability. Thus, fault zones play a crucial role in subsurface hydrocarbon. Therefore, studying the architecture of subsurface fault zone is significant via seismic data for petroleum exploration and production.

The Junggar Basin lies in the northwestern China (Figure 1a), covering approximately an area of 1.3×10^5 km^2. This basin is a triangular basin and lies at the juncture of the Kazakhstan, Siberia, and Tarim cratons. Junggar Basin is bounded by the Kelameili and Qinggelidi Mountains on its northeast side, the Zhayier, Halaalate, and Delun Mountains on its northwest side, and the Yilinheibiergen and Bogeda Mountains on its south side. The studied M17 survey is located in the central part of the Junggar Basin and is one of the most prolific oil and gas exploration areas (Figure 1b). Junggar basin has experienced Hercynian, Indo-Chinese, Yanshan, and Himalayan tectono-sedimentary periods. This basin was filled with the Carboniferous, Permian, Triassic, Jurassic, Cretaceous, Tertiary, and Quaternary strata with thickness up to 14,000 m. It was formed in the Late Carboniferous by the collision and amalgamation of the Central Asian Orogenic Belt. The present study aims to unlock more details of the subsurface fault zone architecture from the 3D seismic data of the M17 survey.

The related research of subsurface fault damage zones adopting 3D seismic data is gradually becoming a hot topic. Conventional seismic attributes are applied to detect the fault zone architecture (Iacopini et al., 2016; Alaei and Torabi, 2017; Ma et al., 2019; Cui et al., 2021). However, the 3D survey containing typical fault linkage types is relative lack. This may further restrict the possible results of the fault zone architecture. The M17 survey from the Junggar Basin contains typical fault zones with different segmented linkage types within the Middle Jurassic Xishanyao Formation (J_2x) map view. Thus, it is logical to consider that this research may probably obtain more findings regarding the architecture of fault zones.

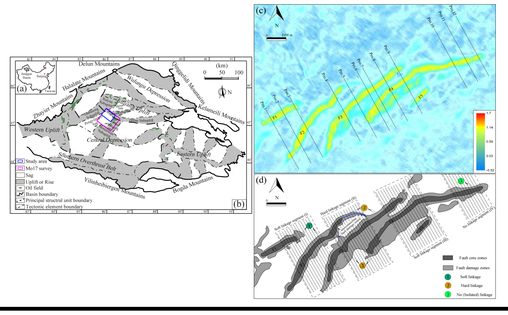

Figure 1 (a) Location of the Junggar Basin in China. (b) Location of M17 3D survey in the Junggar Basin. The M17 survey is marked using a red rectangle, while the studied area is labeled using a blue rectangle. (c) Map of the calculated hybrid attribute of the trimmed zone, including typical fault zone arrays with different segmented linkage types within the studied area. Colors represent extracted hybrid attribute values along the only horizon. This map lies in the southeast part of the study area. The fault zones with fault cores are numbered F1, F2, F3, F4, and F5. (d) Map of the segmented fault zone arrays. They are digitized, according to (c).

Method and Theory

The data adopted in this research are part zone (marked using a blue rectangle in Figure 1b) from the M17 3D seismic survey. The seismic data are sampled at 4 ms and are of moderate quality.

Seismic attributes could be quantitatively used in fault damage zone analysis (Chopra and Marfurt, 2007; Iacopini et al., 2016; Alaei and Torabi, 2017; Zhao et al., 2021). We analyzed the damage zones according to the previous seismic surface attribute methods (Liao et al., 2020). The seismic surface attribute is a hybrid attribute calculated through a supervised multilayer perceptron neural network. Based on the computed hybrid attribute values, the fault damage zones with intense disturbance and discontinuities were interpreted as three levels. Specifically, the zone with high, intermediate, and low hybrid attribute values is respectively regarded as the fault core, damage zone, and protolith zone.

The only horizon within the Middle Jurassic Xishanyao Formation (J_2x) was interpreted. We mainly digitized and labeled five fault zones from that horizon co-rendered with hybrid attributes. Then, hybrid attribute values were measured from the labeled sections perpendicular to the strike of these segmented fault zones.

Result

The features of fault zones were measured along the studied fault zones at the base surface of the coal seam within the Middle Jurassic Xishanyao Formation (J_2x). We mainly studied five major fault zones with NE-SW strike labeled F1–F5 (Figure 1c-d). We exhibited typical sections of the seismic hybrid attribute arranged across all the numbered faults (Figure 1c), covering about four different segmented zones in the map view. According to the existing three styles of fault linkage or overlap, a total of four segmented zones can be divided in the map view in total, namely soft linkage, hard linkage, soft linkage, and (or no) linkage zones (Figure 1d) from SW toward NE.

Herein, the zone with high hybrid attribute values > 0.9 (dark gray in Figure 2) stands for fault cores while the zone with intermediate hybrid attribute values, 0.2 – 0.9 (light gray in Figure 2), represents fault damage zones. The background variance, -0.2 – 0.2 (Figure 2d) refers to protolith zones. These sampled sections reveal different styles of fault zone architecture (Figure 2d). The double-pulse (or multiple-pulse) section of (Figure 2a) contains two large fault cores and four accompanied damage zones that are separated by protolith zones characterized by background hybrid attribute values. The two whole fault zones seem not influenced by each other (Figure 2a). In addition, the pro. 4 in Figure 2b, pro. 8 and pro. 9 in Figure 2c also exhibit double-pulse or three-pulse shapes in the attribute section. The hump section of up to 2400m (pro.7 in Figure 2c) comprises two core zones and three damage zones. The dome sections could be observed, such as the pro. 5 and pro. 6 in Figure 2b. It contains only a thin damage zone with intermediate hybrid attribute values. The fault cores do not develop within them. The single-pulse section (Figure 2d) is a typically isolated damage zone with a central core zone of high hybrid attribute values and two damage zones with intermediate hybrid attribute values (Figure 2d).

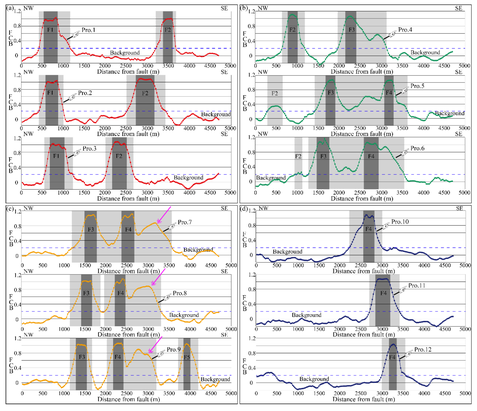

Figure 2 Four section sets of the computed hybrid attribute values across the fault zones; sections locations in Figure 1c; hybrid attribute values above the background marked with light blue dotted lines are interpreted as fault zones. Note the hybrid attribute asymmetry of Figure 2c with a higher hybrid attribute value associated with a newly derived damage zone (marked using pink arrows).

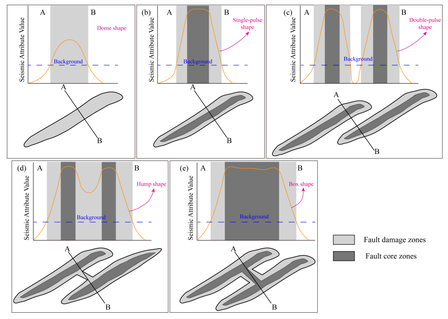

Figure 3 Typical architecture and the corresponding plane distribution of fault zones. Five architectures exhibit different curve characteristics of hybrid seismic attributes (marked with orange color).

According to previous models and the latest results from Figure 2, five typical types of the architecture of the fault zones in total could be summarized: dome shape, single-pulse shape, double-pulse shape, hump shape and box shape (Figure 3a-e).

Conclusions

The latest workflows provided herein more details about the subsurface fault zone, especially the typical types of fault zone architecture. Accordingly, the five typical types of fault zone architecture could be proposed.

Acknowledgement

We thank the PetroChina Xinjiang Oilfield Company for providing the M17 3D survey data.

References

Alaei, B., and A. Torabi, 2017, Seismic imaging of fault damaged zone and its scaling relation with displacement: Interpretation, 5, SP83–SP93.

Caine, J. S., J. P. Evans, and C. B. Forster, 1996, Fault zone architecture and permeability structure: Geology, 24, 1025–1028.

Chopra, S., and K. Marfurt, 2007, Curvature attribute applications to 3D surface seismic data: Leading Edge (Tulsa, OK), 26, 404–414.

Cui, L., S. Jian, B. Zhang, X. Xie, and L. I. Liang, 2021, Distribution of Mid-deeply Buried Sand-bodies and their Hydrocarbon Significance at Basin Margins: Case Study of the Paleogene in the Eastern Liuzan Area of the Nanpu Sag, Bohai Bay Basin, China: Acta Geologica Sinica, 95, 1279–1294.

Iacopini, D., R. W. H. Butler, S. Purves, N. McArdle, and N. De Freslon, 2016, Exploring the seismic expression of fault zones in 3D seismic volumes: Journal of Structural Geology, 89, 54–73.

Liao, Z., W. Li, H. Zou, F. Hao, K. J. Marfurt, and Z. Reches, 2020, Composite damage zones in the subsurface: Geophysical Journal International, 222, 225–230.

Ma, D. B., G. H. Wu, N. Scarselli, X. S. Luo, J. F. Han, and Z. Y. Chen, 2019, Seismic damage zone and width–throw scaling along the strike-slip faults in the Ordovician carbonates in the Tarim Basin: Petroleum Science, 16, 752–762.

Zhao, Z., J. Liu, W. Ding, R. Yang, and G. Zhao, 2021, Analysis of seismic damage zones: A case study of the ordovician formation in the shunbei 5 fault zone, tarim basin, China: Journal of Marine Science and Engineering, 9, 630.

中国石油大学(北京)克拉玛依校区 CHINA UNIVERSITY OF PETROLEUM - BEIJING AT KARAMAY

Lijie Cui
lijiecui2020@outlook.com